Distinct roles and synergistic function of Fru^{M} isoforms in *Drosophila* olfactory receptor neurons

Ye Zhang[1], **Renny Ng**[1], **Megan C. Neville**[2], **Stephen F. Goodwin**[2], **Chih-Ying Su**[1,*]

[1]Neurobiology Section, Division of Biological Sciences, University of California San Diego, La Jolla, CA 92093, USA

[2]Centre for Neural Circuits and Behaviour, University of Oxford, Oxford OX1 3TA, UK

SUMMARY

Sexual dimorphism in *Drosophila* courtship circuits requires the male-specific transcription factor *fru^{M}*, which is alternatively spliced to encode the Fru^{MA}, Fru^{MB} and Fru^{MC} isoforms. Most *fru^{M}*-positive neurons express multiple variants; however, the functional significance of their co-expression remains undetermined. Do co-expressed isoforms each play unique roles to jointly regulate dimorphism? By focusing on *fru^{M}*-positive olfactory receptor neurons (ORNs), here we show that Fru^{MB} and Fru^{MC} are both required for males' age-dependent sensitization to aphrodisiac olfactory cues in a cell-autonomous manner. Interestingly, Fru^{MB} expression is upregulated with age in Or47b and Ir84a ORNs, and its overexpression mimics the effect of age in elevating olfactory responses. Mechanistically, Fru^{MB} and Fru^{MC} synergistically mediate response sensitization through cooperation of their respective downstream effectors, namely, PK25 and PPK23, which are both required for forming a functional amplification channel in ORNs. Together, these results provide critical mechanistic insight into how co-expressed Fru^{M} isoforms jointly coordinate dimorphic neurophysiology.

INTRODUCTION

In *Drosophila*, sexual dimorphism is determined by genes that regulate the alternative splicing of male- or female-specific transcription factors. In particular, the male products of the *fruitless* gene (Fru^{M}) play essential roles in determining dimorphic neural circuits (for reviews, see Billeter et al., 2006a; Dickson, 2008; Pavlou and Goodwin, 2013; Sato et al., 2020; Yamamoto and Koganezawa, 2013). The *fru^{M}* transcript is further subject to alternative splicing at its 3' end, yielding three functional variants, namely, Fru^{MA}, Fru^{MB}, Fru^{MC} (Demir and Dickson, 2005; von Philipsborn et al., 2014; Song et al., 2002) — also known as Fru^{AM}, Fru^{EM}, and Fru^{BM}, respectively (Nojima et al., 2014; Sato and Yamamoto, 2020; Usui-Aoki et al., 2000). Each isoform contains a common N-terminal BTB protein

DECLARATION OF INTERESTS

The authors declare no competing interests.

dimerization domain and a unique zinc finger DNA-binding domain, and all three are predicted to function as transcription factors (Billeter et al., 2006b; Meissner et al., 2016; Neville et al., 2014; von Philipsborn et al., 2014; Ryner et al., 1996). Although RNAseq, ChIP-seq or genomic occupancy analysis of cells ectopically expressing Fru^{MA}, Fru^{MB}, or Fru^{MC} reveals unique DNA binding sites for each variant, the three isoforms nevertheless appear to target overlapping sets of genes involved in neural development, synaptic transmission, or ion channel signaling (Dalton et al., 2013; Neville et al., 2014; Vernes, 2014).

At the cellular level, Fru^{MB} and Fru^{MC} are largely co-expressed, whereas Fru^{MA} is found in the smallest subset of fru^{M+} neurons (Neville et al., 2014; Nojima et al., 2014; von Philipsborn et al., 2014). Despite their overlapping expression, the isoforms are likely non-redundant in function. Among the three isoforms, Fru^{MC} is known to play a central role in male sexual behavior (Billeter et al., 2006b; Neville et al., 2014; von Philipsborn et al., 2014) and is also necessary for development of the male-specific muscle of Lawrence (MOL); in fru^{M} or fru^{MC} mutants, MOL induction can only be rescued by Fru^{MC}, but not Fru^{MA} or Fru^{MB}, indicating that Fru^{MC} cannot be substituted by the other Fru^{M} isoforms in this context (Billeter et al., 2006b). Furthermore, the mAL/aDT2, aSP4 and vAB3 neural clusters all expressly require Fru^{MC} for male-specific neurite arborizations, despite the co-expression of other Fru^{M} isoforms (von Philipsborn et al., 2014). Mechanistically, Fru^{MC} orchestrates mAL neurons' dimorphic development through interacting with other transcription or chromatin regulators to repress the expression of the axon guidance molecule *robo1* (Chowdhury et al., 2017; Ito et al., 2016; Sato and Yamamoto, 2020). The aforementioned examples suggest that Fru^{M} isoforms play distinct roles in both behavior and neurodevelopment. However, it remains unclear whether the isoforms operate beyond these contexts. It is also unknown whether all isoforms exhibit specific cellular functions, or in which neuronal population these functions are fulfilled. Addressing these questions is essential for understanding why multiple isoforms are typically co-expressed and how isoform-specific functions influence dimorphic circuits.

Co-expressed isoforms may also perform cooperatively. In fru^{M} mutant males, whose serotonergic-abdominal giant neurons (s-Abg) are less numerous and display female-like neurite morphology (Lee and Hall, 2001), genetic rescue with Fru^{MB} or Fru^{MC} only partially restores the male-specific features, while Fru^{MA} does not alleviate the mutant phenotype (Billeter et al., 2006b). These observations indicate that neither Fru^{MB} nor Fru^{MC} alone is sufficient to confer the full male-specific complement of s-Abg neurons, suggesting that in this context, there is synergistic function between the Fru^{M} isoforms (Neville et al., 2014). But insofar as the mechanism of cooperativity is unidentified, how different Fru^{M} isoforms operate synergistically remains an outstanding question.

Intriguingly, Fru^{M} is expressed well into adulthood (Hueston et al., 2016; Neville et al., 2014; von Philipsborn et al., 2014), suggesting that the isoforms may function beyond regulating neurodevelopment. What roles do they play in adult neurons? Might they underlie dimorphic neurophysiology, i.e. neural response properties? Indeed, a previous study shows that Fru^{M} is required for social context to influence male-specific neurophysiology (Sethi et al., 2019). Of note, dimorphic response properties has been reported in the courtship-

promoting Or47b and Ir84a ORNs, which express Fru^M, and whose responses become more sensitive with age in males but not females (Lin et al., 2016; Ng et al., 2019; Stockinger et al., 2005). This age-dependent sensitization markedly impacts courtship behavior and is regulated by a reproductive hormone — juvenile hormone — through upregulation of Pickpocket 25 (PPK25), an obligate subunit of a Degenerin/Epithelial sodium channel (DEG/ENaC) amplification channel (Lin et al., 2016; Ng et al., 2019). Notably, juvenile hormone signaling also regulates male fertility (Wilson et al., 2003). Thus, dynamic modulation of olfactory sensitivity allows a single hormone to coordinate sexual behavior with reproductive maturity, a strategy also observed in female mice (Dey et al., 2015). Given the behavioral significance of age-dependent sensitization, which Fru^M isoform(s) are required for the male-specific regulation of olfactory neurophysiology? Is there a hierarchical relationship between Fru^M isoforms, PPK25 and juvenile hormone signaling? If multiple isoforms are involved, do they collaborate directly to modulate common downstream targets; or do different effectors, regulated by their respective isoform, act cooperatively instead?

In this study, we begin by systematically analyzing the functions and expression patterns of all three Fru^M isoforms in ORNs. We identify unique roles for co-expressed Fru^M isoforms in courtship-promoting ORNs and uncover a molecular mechanism whereby multiple Fru^M isoforms cooperate to mediate the neurons' age-dependent sensitization. Specifically, both Fru^{MB} and Fru^{MC} are required for the elevated Or47b responses of older males. When overexpressed, only Fru^{MB} can mimic the effects of age in sensitizing Or47b ORN responses, consistent with our finding that expression of Fru^{MB} alone shows age-dependent upregulation. Through a series of epistasis experiments, we show that Fru^{MB} operates downstream of juvenile hormone signaling and upstream of PPK25 expression. Interestingly, although Fru^{MC} is not upregulated with age, its downstream target, PPK23, is also required for PPK25 to form an amplification channel. These results illustrate how functional synergy between Fru^{MB} and Fru^{MC} can be achieved: through cooperation of their respective downstream targets. Furthermore, we show that neuronal identity determines the synergy, which is conserved between courtship-promoting Or47b and Ir84a neurons but absent in the courtship-inhibiting Or67d ORNs. By focusing on the Or47b ORN, a representative Fru^M-positive and dimorphic neuron, this study furthers our understanding of how co-expressed Fru^M isoforms can regulate sexually dimorphic neurophysiology in a coordinated manner.

RESULTS

Fru^M is necessary for age-dependent olfactory sensitization

Among the three types of fru^{M+} ORNs in the male antenna, the courtship-promoting Or47b and Ir84a neurons exhibit age-dependent response increases, while the courtship-inhibiting Or67d neurons do not alter sensitivity with age (Lin et al., 2016; Ng et al., 2019). We first surveyed whether Fru^M influences the responses of these ORNs to their ligands: the Or47b receptor responds to palmitoleic acid (Lin et al., 2016), Ir84a to phenylacetaldehyde (Grosjean et al., 2011) and Or67d to *cis*-vaccenyl acetate (van der Goes van Naters and Carlson, 2007; Kurtovic et al., 2007; Tal and Smith, 2006). Using single-sensillum recording, we found that the age-dependent sensitization of Or47b ORNs (Figure 1A) was

abolished in fru^F mutant males, which do not express any functional Fru^M proteins (Demir and Dickson, 2005) (Figure 1B). On the other hand, the loss of Fru^M did not affect the Or47b olfactory responses of 2-day old males (Figure 1C), suggesting that Fru^M is dispensable for the ORNs' baseline pheromone response.

Similarly in the Ir84a neurons, Fru^M was only required for the elevated olfactory responses of 7-day-old males (Figures 1D–F). Meanwhile, neither age nor Fru^M influenced Or67d ORN responses (Figures 1G–I). Together, these results indicate that Fru^M is selectively required for age-dependent sensitization in the courtship-promoting Or47b and Ir84a ORNs (Figure 1J).

Fru^{MB} and Fru^{MC} are both required for age-dependent olfactory sensitization

To determine which Fru^M isoform is necessary for age-dependent sensitization, we examined isoform-specific mutant males heterozygous for the fru^F allele and the fru^A, fru^B or fru^c mutant allele (Billeter et al., 2006b; Neville et al., 2014) (Figure 2A). We found that the Or47b ORN responses from 7-day-old fru^{MA} mutants (fru^A/fru^F) remained significantly higher than those from 2-day-olds (Figure 2B). Specifically, both response magnitudes and age-dependent sensitization were unaffected in fru^{MA} mutants, which remained indistinguishable from controls (fru^A/+) (Figure 2C). These results indicate that Fru^{MA} does not underlie the elevated Or47b olfactory responses in 7-day old males, and that age-dependent sensitization persists in males carrying single copies of fru^M allele in the fru^A/fru^F mutant flies. We note that in heterozygous mutants, significant age-dependent sensitization was only observed at the highest dose of palmitoleic acid applied (10^{-1}, Figure 2B) when compared to wildtype controls (Figure 1A). This difference likely arises from Fru^M heterozygosity, which may reduce the range of Or47b ORN sensitization due to haploinsufficiency, as previously observed (Sethi et al., 2019).

Meanwhile in fru^{MB} or fru^{MC} mutant males (fru^B/fru^F or fru^C/fru^F), the Or47b ORN responses of 7-day-olds were reduced and resembled those of 2-day-olds (Figures 2D–G), indicating that Fru^{MB} and Fru^{MC} are both necessary for age-dependent sensitization. To further determine whether these Fru^M proteins operate in a cell-autonomous manner, we employed isoform-specific micro RNAi lines (von Philipsborn et al., 2014) to selectively knock down either Fru^{MB} or Fru^{MC} in the Or47b ORNs, and also observed abolishment of age-dependent sensitization (Figure S1). Of note, our genetic manipulations abolished the expression of both the targeted Fru^M isoform and the corresponding Fru^{COM} variant that are commonly expressed in both sexes. However, given that Fru^{COM} functions mainly during early development and is not expressed in the adults (Song et al., 2002), our observed phenotypes likely arose entirely through deficiency in a specific Fru^M isoform. Taken together, these results show that both Fru^{MB} and Fru^{MC}, but not Fru^{MA}, are required for the elevated Or47b olfactory responses in older males (Figure 2H).

Fru^M isoforms are differentially regulated with age in courtship-promoting ORNs

Given that Or47b ORN sensitization requires Fru^{MB} and Fru^{MC}, how are these factors related with age? We postulated that the expression of specific Fru^M isoforms is dynamically regulated. To test this hypothesis, we examined published isoform reporter lines in which the

C-terminus of an individual alternative exon (A, B or C) is tagged with a c-*myc* epitope, allowing labeling of the male-specific Fru^M isoforms as well as the Fru^{COM} isoforms (von Philipsborn et al., 2014). With immunohistochemistry, we first determined that all three isoforms are expressed in the Or47b ORNs of male but not female flies (Figure 3 and data not shown), confirming that only Fru^M isoforms, instead of Fru^{COM}, were detected in this assay.

As expected, Fru^M expression changed in an age- and isoform-dependent manner (Figure 3). In *fru^{A-myc}* males, the *myc* immunofluorescence levels in Or47b ORNs of 7-day-old males were lower than that of 2-day-olds, indicating downregulated Fru^{MA} expression (Figures 3A and 3B). In contrast, there was marked increase in Fru^{B-myc} expression (Figures 3C and 3D). Finally, we observed an age-dependent decrease in Fru^{C-myc} expression in Or47b ORNs (Figures 3E and 3F). Together, these results demonstrate that in male Or47b ORNs, all three Fru^M isoforms are expressed, and that Fru^{MB} protein expression is upregulated with age, while Fru^{MA} and Fru^{MC} are downregulated (Figure 3G).

Because Ir84a and Or67d ORNs also express Fru^M, we examined isoform-specific expression in these neurons as well. We observed a similar trend of Fru^{MB} upregulation and Fru^{MC} downregulation in the Ir84a ORNs (Figure S2A). Interestingly in the Or67d neurons, although all three isoforms were detected, their expression remained unchanged with age (Figure S2B). In summary, our systematic survey shows that Fru^M isoforms are differentially regulated with age in the courtship-promoting ORNs, and that a common pattern of isoform-specific modulation — Fru^{MB} upregulation and Fru^{MC} downregulation — may mediate the sensitization of Or47b and Ir84a neurons.

Overexpression of Fru^{MB} elevates male Or47b ORN responses

Given the isoform-specific modulation (Figure 3), how might overexpression of an individual isoform affect Or47b ORNs? Can this manipulation mimic age in elevating olfactory responses? To address these questions, we employed the GAL4-UAS system to overexpress a single Fru^M isoform in the Or47b ORNs of 2-day old males. Fru^{MA}-overexpression did not alter neuronal responses compared to controls (Figures 4A and 4B), which is in agreement with Fru^{MA}'s dispensability for Or47b response regulation (Figure 2B). On the other hand, Fru^{MB} overexpression markedly increased the neuronal responses (Figures 4C and 4D), supporting the notion that age — through Fru^{MB} upregulation — drives the response increase in Or47b neurons.

Furthermore, we examined whether increased Fru^{MB} expression also underlies Ir84a response sensitization, and found that its overexpression similarly elevated the responses in 2-day old males (Figures S3A and S3B). In comparison, Fru^{MB} overexpression in Or67d ORNs unexpectedly abolished their olfactory responses (Figures S3C and S3D), indicating that upregulation of Fru^{MB} does not invariably elevate responses in all *fru^{M+}* ORN types. It is plausible that additional transcription factors — likely partnering with Fru^{MB} — are involved in selecting the isoform's target genes that either sensitize responses in Or47b and Ir84a neurons or inhibit responses in Or67d ORNs.

Lastly, we examined the impact of Fru^{MC} overexpression on Or47b ORN responses. Consistent with its lack of upregulation (Figure 3F), increasing Fru^{MC} expression in Or47b neurons did not elevate responses (Figure 4E). Instead, this manipulation reduced olfactory sensitivity (Figure 4F), raising the possibility for opposing functions of Fru^{MB} and Fru^{MC} (see Discussion). In all, our overexpression experiments show that upregulation of Fru^{MB}, but not Fru^{MA} or Fru^{MC}, in the courtship-promoting ORNs can confer elevated olfactory responses (Figure 4G).

Fru^{MB} is downstream of juvenile hormone signaling and upstream of PPK25 expression in male Or47b neurons

Previous work shows that Fru^{M} expression in the antennae of 7-day old males requires *methoprene-tolerant* (*Met*) (Sethi et al., 2019), a juvenile hormone receptor (Jindra et al., 2013; Wilson and Fabian, 1986). Moreover, juvenile hormone signaling drives the upregulation of PPK25, a DEG/ENaC member which amplifies olfactory inputs in the courtship-promoting ORNs and whose antennal expression level increases with age in males (Ng et al., 2019). Eliminating Met, Fru^{M}, or PPK25 abolishes age-dependent sensitization (Lin et al., 2016; Ng et al., 2019) (Figure 1). Conversely, heightened Met signaling or overexpressing Fru^{MB} or PPK25 in the Or47b ORNs increases their pheromone responses (Lin et al., 2016; Ng et al., 2019; Sethi et al., 2019) (Figure 4D). These observations suggest that these molecules function in the same pathway to increase Or47b olfactory responses. However, it was unclear how Fru^{MB} operates within this hierarchy.

To establish the relationship between Fru^{MB} and juvenile hormone signaling, we performed epistasis experiments by overexpressing Fru^{MB} in the Or47b ORNs of *Met* mutants. If Fru^{MB} is downstream of Met, we expect this manipulation to elevate Or47b olfactory responses, as in a wildtype background (Figure 4D). Indeed, Fru^{MB} overexpression markedly increased Or47b ORN response despite the absence of Met (Figures 5A and 5B), implying that Fru^{MB} is downstream of juvenile hormone signaling.

We next determined the relationship between Fru^{MB} and PPK25 by overexpressing Fru^{MB} in the Or47b ORNs of *ppk25* mutant males (Lin et al., 2005). This manipulation failed to elevate their Or47b olfactory responses (Figures 5C–D), suggesting that Fru^{MB} requires functional PPK25 to sensitize the ORNs and, regarding the isoform's hierarchical position, that Fru^{MB} operates upstream of PPK25. Together, these results (Figures 5E–G) support a model whereby 1) Fru^{MB} is upregulated with age via juvenile hormone signaling in male Or47b ORNs, and 2) Fru^{MB} further drives the expression of PPK25, which in turn amplifies the olfactory responses of these neurons (Figure 5H).

Fru^{MB} and Fru^{MC} cooperatively elevate Or47b ORN responses through distinct downstream effectors

Given that Fru^{MB} and Fru^{MC} are both required for age-dependent sensitization (Figure 2), we asked how these isoforms cooperate to modulate neurophysiology. We note that overexpression of PPK25 alone in male Or47b ORNs is sufficient to confer increased responses; however, the same manipulation in females fails to elevate olfactory output (Ng et al., 2019). These observations suggest that PPK25 by itself cannot form a functional DEG/

ENaC channel, which is typically composed of three subunits (Hanukoglu and Hanukoglu, 2016; Kellenberger and Schild, 2002; Staruschenko et al., 2005). Therefore, the normal function of PPK25 likely requires at least another DEG/ENaC subunit that is also expressed in male Or47b neurons.

To identify PPK25's partner, we followed a candidate-based approach by focusing on another DEG/ENaC subunit, named PPK23, which is expressed together with PPK25 in a subset of fru^{M+} tarsal gustatory neurons for the detection of aphrodisiac contact pheromones (Liu et al., 2018; Pikielny, 2012; Thistle et al., 2012; Toda et al., 2012). We postulated that a similar PPK23-PPK25 partnership also exists in Or47b ORNs, where both subunits are required to form a functional amplification channel. Indeed in *ppk23* mutant males, age-dependent sensitization was no longer observed (Figures 6A–B), as in *ppk25* mutants (Ng et al., 2019). Quantification of the responses indicates that loss of *ppk23* did not abolish Or47b pheromone responses, but reduced them to the 2-day old wildtype level (Figure 6C). These results support PPK23's functional role as a subunit of the amplification channel in Or47b ORNs. We note, however, that *ppk23* transcript levels in the antenna were extremely low (<1 FPKM in 2-day or 7-day old male antennal RNAseq, not shown), and that a characterized *ppk23-GAL4* driver (Thistle et al., 2012) did not label Or47b ORNs (not shown). A possible explanation is that mRNA transcript levels do not always reflect degrees of protein expression, which is the case for another antennal gene—*Ir93a*—whose transcript levels are extremely low but whose protein is expressed in subsets of antennal neurons (Knecht et al., 2016; Menuz et al., 2014).

Might a specific Fru^M isoform regulate PPK23 or PPK25? This inquiry is important in the context of a critical question: at which level do co-expressed Fru^{MB} and Fru^{MC} cooperatively mediate Or47b response sensitization? One possible model is that Fru^{MC} collaborate with Fru^{MB} to regulate the expression of both PPK23 and PPK25 (Figure 7A, Model I). Alternatively, Fru^{MB} and Fru^{MC} may operate as independent transcription regulators, each driving the expression of a distinct downstream effector. In this scenario, Fru^{MB} is likely directly upstream of PPK25, given that both molecules are upregulated with age (Ng et al., 2019) (Figure 3D); Fru^{MC} might then be required for the expression of PPK23, independent from the Fru^{MB}/PPK25 pathway (Figure 7A, Model II). To distinguish between these two possibilities, we targeted female Or47b neurons for genetic manipulations, taking advantage of their lack of Fru^M isoform or the amplification channel (Ng et al., 2019). Consistent with the functional requirement of Fru^{MC} (Figure 2), ectopic expression Fru^{MB} alone in female Or47b ORNs did not elevate their pheromone responses (Figure 7B). In contrast, co-expression of Fru^{MB} and Fru^{MC} markedly heightened female responses (Figure 7C), indicating that Fru^{MB} and Fru^{MC} together can confer Or47b olfactory sensitization. In comparison, expression of both Fru^{MB} and Fru^{MA} in female Or47b neurons did not affect responses (Figure S4).

According to model I, because both Fru^{MB} and Fru^{MC} are required to regulate PPK23 and PPK25, overexpressing PPK25 in female neurons together with a single Fru^M isoform is not expected to yield response changes. On the other hand, if Model II is correct, expressing PPK25 with Fru^{MB} also will not yield increased responses, because Fru^{MB} and PPK25 operate in the same pathway. However, expressing PPK25 along with Fru^{MC}, which

regulates a different downstream effector, should now mimic the effect of Fru[MB] and Fru[MC] co-expression (Figure 7C), and subsequently elevate the Or47b olfactory responses in females.

In support of model II, we observed a marked increase in Or47b responses when PPK25 (Vijayan et al., 2014) and Fru[MC] were co-expressed (Figure 7D). Moreover, we found that expression of PPK25 together with Fru[MB] failed to confer sensitization (Figure 7E), further supporting Model II in which these two molecules operate in the same pathway. This result also agrees with the previous finding that overexpression of PPK25 alone cannot elevate female Or47b ORN responses (Ng et al., 2019); in both cases, PPK25 lacked its partner, PPK23. Further, based on published bioinformatics studies (Dalton et al., 2013; Neville et al., 2014), we identified putative Fru[MB] DNA binding domains upstream of *ppk25* (Figure S5), suggesting that Fru[MB] may directly mediate *ppk25* upregulation. In all, these results show that each of the Fru[M] isoforms has its own unique downstream target(s) in Or47b ORNs (Figure 7A, Model II).

As predicted by Model II, ectopic expression of PPK23 with Fru[MC] in female Or47b ORNs yielded no response increase (Figure 7F), suggesting that these molecules could operate in the same pathway. Consistent with this notion, we also identified putative Fru[MC] DNA binding domains upstream of *ppk23* (Figure S5). On the other hand, expressing PPK23 together with Fru[MB] markedly increased the pheromone responses (Figure 7G), mimicking Fru[MC]/Fru[MB] co-expression (Figure 7C). Together, these results strongly support a model whereby Fru[MB] and Fru[MC] respectively mediate the expression of PPK25 and PPK23, of which both are required to form an amplification channel that sensitizes Or47b ORN responses. Overall, co-expressed Fru[MB] and Fru[MC] coordinate dimorphic neurophysiology at the level of their unique downstream effectors.

Fru[MA] is required for the enlargement of all three sexually-dimorphic glomeruli

Having determined the roles of Fru[MB] and Fru[MC] in Or47b neurophysiology (Figure 2), we next investigated the function of Fru[MA]. Previous work shows that the male VA1lm glomerulus — innervated by Or47b ORNs — exhibits sexually dimorphic enlargement, and that volumetric difference depends on Fru[M] expression (Stockinger et al., 2005). Given Fru[MA]'s dispensability for olfactory sensitization (Figure 2B), we wondered whether the isoform might instead be required for male-specific glomerular enlargement.

To test this possibility, we quantified the sizes of VA1lm in wildtype and different *fru[M]* mutant backgrounds. Consistent with the published phenotype (Stockinger et al., 2005), eliminating the expression of all three Fru[M] isoforms by disrupting the P1 promoter (*fru[GAL.4.P1]*) markedly reduced the size of male VA1lm, when compared to the heterozygous controls (Figure S6A, first and second panels). Interestingly, select disruption of either Fru[MA] or Fru[MC] — but not Fru[MB] — also resulted in a similar reduction in the VA1lm size (Figure S6A), supporting a functional role of these two isoforms in male-specific enlargement of this glomerulus. As negative controls, we performed the same analysis in females and found that their VA1lm sizes were essentially the same across all genotypes tested (Figure S6B).

In addition, we examined the VL2a and DA1glomeruli, which are innervated by Ir84a and Or67d ORNs, respectively. To facilitate a comparison, we normalized the glomerular volumes of males to those of females, indicated as the volume ratio between sexes (Figure S6C). Elimination of Fru^{MA} similarly downsized these two glomeruli in males, while Fru^{MB} did not influence glomerular volumes. Finally, Fru^{MC} plays a distinct role in each glomerulus: mutation of this isoform reduced the size of VA1lm, left VL2a volume unchanged, and increased DA1 volume (Figure S6C). Collectively, these results point to a role of Fru^{MA} in mediating the sexually-dimorphic enlargement of fru^{M+} glomeruli in males (Figure S6D).

DISCUSSION

In this study, we systematically characterized the functions of all three Fru^M isoforms in regulating male-specific olfactory neurophysiology and glomerular morphology. We showed that Fru^{MA}, Fru^{MB}, and Fru^{MC} are expressed and differentially regulated with age in the Or47b ORNs (Figure 3) — which are representative fru^{M+} and sexually dimorphic sensory neurons — and that each isoform plays distinct roles in mediating dimorphism. Specifically, we found that Fru^{MA} is required for these neurons' male-specific glomerular enlargement (Figure S6), while Fru^{MB} and Fru^{MC} cooperate to mediate ORNs' age-dependent sensitization in a cell-autonomous manner (Figure 2).

Notably, our study uncovers a functional role for Fru^{MA}, whose importance in sexual dimorphism has not been characterized (Billeter et al., 2006b; Neville et al., 2014; Nojima et al., 2014; von Philipsborn et al., 2014; Wohl et al., 2020). Our finding on Fru^{MA} contrasts with previous studies identifying Fru^{MC} as the dominant isoform in regulating male-specific neural morphology: specifically, the innervation patterns as observed in the s-Abg serotonergic neurons, or the mAL/aDT2, aSP4 and vAB3 neural clusters (Billeter et al., 2006b; von Philipsborn et al., 2014). These observations illustrate that sexually dimorphic neuroanatomy requires different Fru^M isoforms in a neuronal-type-dependent manner. An interesting direction for future research will be to determine whether Fru^{MA} operates in a cell-autonomous manner in fru^{M+} ORNs, what cellular determinants underlie enlarged glomeruli, and how Fru^{MA} regulates the number of neurons and/or neurite growth during pupal development.

Fru^M proteins contain a BTB domain, a conserved protein-protein interaction module able to both self-associate and interact with other proteins (Sato and Yamamoto, 2020; Sato et al., 2019; Stogios et al., 2005). Fru^{MC}, for example, is able to recruit other transcription or chromatin regulators to modulate dimorphic neurite morphology (Chowdhury et al., 2017; Ito et al., 2012; Sato and Yamamoto, 2020). Intriguingly, Fru^{MB} and Fru^{MC} are commonly co-expressed and can perform synergistically (Billeter et al., 2006b; Neville et al., 2014; von Philipsborn et al., 2014). However, it has been unclear whether functional synergism between isoforms arises from their direct dimerization or through other means. Here we show that in Or47b ORNs, Fru^{MB} and Fru^{MC} independently regulate distinct downstream effectors, PPK25 and PPK23, which then cooperate to elevate Or47b pheromone responses (Figures 7). Prior to this study, the individual downstream targets for co-expressed Fru^M isoforms within a single cell have never been characterized. Our results now suggest that in

neurons expressing multiple splice variants, each isoform may specifically target unique effector genes, which in turn interact with each other to function cooperatively. Through future research, it will be important to determine whether this logic is conserved in other neurons expressing alternatively spliced isoforms of transcription factors.

Unexpectedly, we found that the expression of individual isoforms is differentially regulated with age in an ORN-dependent manner (Figures 3 and S2). In the courtship-promoting ORNs, we observed a concomitant Fru^{MB} upregulation and Fru^{MC} downregulation. This isoform-specific regulation is functionally relevant, as overexpression of Fru^{MB} can elevate responses in Or47b and Ir84a ORNs, mimicking the effect of age. On the other hand, the effects of Fru^{MB} overexpression depend on ORN identity as this manipulation instead abolished the olfactory responses of Or67d ORNs (Figures S3C–D). These findings indicate that upregulation of Fru^{MB} does not invariably elevate responses in all ORN types, and that Fru^{MB} targets distinct downstream effectors in the courtship-promoting and courtship-inhibiting ORNs. A given Fru^{M} isoform may up- or down-regulate varying target genes in different cells, likely through partnering with distinct transcription factors. Consistent with this idea, Or67d ORNs do not express PPK25 nor exhibit age-dependent sensitization (Lin et al., 2016; Starostina et al., 2012), despite their expression of both Fru^{MB} and Fru^{MC} isoforms (Figure S2B). Our results thus highlight the nuanced, non-binary regulation of Fru^{M} isoforms, a sophisticated mechanism which affords the Fru^{M} proteins versatility in their functional output.

What is the biological significance of the opponent modulation with coincident Fru^{MB} upregulation and Fru^{MC} downregulation (Figures 3 and S2)? Channel stoichiometry may provide the answer. PPK25 and PPK23, the isoforms' respective downstream effectors, are members of the DEG/ENaC family whose cation channels are composed of three subunits (Hanukoglu and Hanukoglu, 2016; Kellenberger and Schild, 2002; Staruschenko et al., 2005). When ectopically expressed, PPK25 alone cannot enhance female Or47b ORN responses (Ng et al., 2019), indicating that PPK25 does not form a functional homotrimeric channel. In contrast, overexpression of PPK25 in the Or47b ORNs of 2-day old males can markedly increase their olfactory responses (Ng et al., 2019), likely due to the presence of PPK23. As such, the opponent modulation of Fru^{MB} and Fru^{MC} is best explained within the scenario in which the functional amplification channel adopts a stoichiometry whereby PPK23/PPK25 ratio is 1:2. In 2-day old males, Fru^{MC} expression is not yet downregulated and Fru^{MB} levels are still low (Figures 3 and S2), likely resulting in higher PPK23 expression relative to PPK25 in the courtship-promoting ORNs. In this scenario, the trimeric channel may fail to assemble, or adopt a nonfunctional or low-conductance stoichiometry (PPK23/PPK25 ratio 2:1 or 3:0); both cases will prohibit response amplification. When male flies are 7 days old, on the other hand, the ratio of Fru^{MB}/Fru^{MC} increases and thus allows PPK25 to be expressed at a higher level than PPK23, favoring the formation of functional amplification channels.

In addition to the aforementioned mechanism, the opponent regulation of Fru^{MB} and Fru^{MC} may further control the PPK25/PPK23 ratio via other means. Upstream of the *ppk25* gene, we identified not only Fru^{MB} DNA binding domains, but also a putative Fru^{MC} binding site (Figure S5), thus raising the possibility that Fru^{MC} may also play a role in modulating *ppk25*

expression. Notably, overexpressing Fru^{MC} in the Or47b ORNs reduced their pheromone responses (Figure 4F), which is opposite to the response-enhancing effect of Fru^{MB} (Figure 4D). It is therefore possible that apart from promoting *ppk23* expression, Fru^{MC} also reduces *ppk25* expression by operating as a transcription inhibitor (Chowdhury et al., 2017; Ito et al., 2016; Sato and Yamamoto, 2020). Thus, the coordinated up- and down-regulation of Fru^{MB} and Fru^{MC} may further ensure the desired PPK25/PPK23 ratio through the isoforms' antagonist impacts on *ppk25* expression.

In summary, our research has identified a mechanism by which multiple Fru^M isoforms cooperatively mediate sexual dimorphism. By focusing on courtship-promoting *fru^{M+}* ORNs that exhibit male-specific neurophysiology and glomerular enlargement, this study uncovers how the chemosensory and morphological aspects of sexual dimorphism may be coordinated through differential regulations of the co-expressed splice variants, and through the synergistic cooperation of these isoforms' downstream effectors.

STAR METHODS

RESOURCE AVAILABILITY

Lead Contact—Further information and requests for resources and reagents should be directed to and will be fulfilled by the Lead Contact, Chih-Ying Su (c8su@ucsd.edu).

Materials Availability—The fly lines generated in this study are available from the Lead Contact.

Data and Code Availability—All software used in this study is listed in the Key Resources Table. Raw data are available upon request.

EXPERIMENTAL MODEL AND SUBJECT DETAILS

***Drosophila* stocks**—All flies (*Drosophila melanogaster*) were raised on standard cornmeal medium at 25°C, ~60% relative humidity in an incubator with a 12-hr light/dark cycle. Flies were collected upon eclosion, separated by sex and raised in groups of 10. Naïve male flies 2 or 7 days post-eclosion were used in all experiments unless noted otherwise. For further information on genotypes, refer to Table S1.

METHOD DETAILS

Single-sensillum recordings—A fly was wedged into the narrow end of a truncated plastic 200-μl pipette tip to expose the antenna, which was then stabilized between a tapered glass microcapillary and a coverslip covered with double-sided type. Single-unit recordings were performed essentially as described (Ng et al., 2017). Briefly, electrical activity of target ORNs was recorded extracellularly by placing a sharp electrode filled with artificial hemolymph solution (Wang et al., 2003) in the at4 sensillum (Or47b ORN recordings). For at1 (Or67d ORN) or ac4 (Ir84a ORN) sensillum recordings, 0.6X sensillum lymph Ringer solution (Kaissling, K. E., Thorson, 1980) was used instead. The reference electrode filled with the same solution was placed in the eye. No more than three sensilla from the same antenna were recorded per fly.

AC signals (100–20k Hz) were recorded on an NPI EXT-02F amplifier (ALA Scientific Instruments) and digitized at 5 kHz with Digidata 1550 (Molecular Devices). ORN spikes were detected and sorted using threshold search under Event Detection in Clampfit 10.4 (Molecular Devices). Spike timing data were exported and analyzed in Igor Pro 6.3 (Wavemetrics). Peri-stimulus time histograms (PSTHs) were obtained by averaging spike activities in 50-ms bins and smoothed using a binomial filter (Igor Pro 6.3, Wavemetrics). For dosage curves and statistical analysis, responses were quantified by subtracting the pre-stimulus spike rate (1 s) from the peak spike frequency during odorant stimulation (adjusted peak responses).

The at4 sensillum, which houses the Or47b ORNs (at4A), was identified based on the location of the sensillum on the antenna, sensillum morphology and the number of compartmentalized neurons, as described (Ng et al., 2017). Or67d ORNs are singly-housed in the at1 sensilla, which were similarly identified in addition to their responsiveness to *cis*-vaccenyl acetate (van der Goes van Naters and Carlson, 2007; Kurtovic et al., 2007; Tal and Smith, 2006). The identity of the ac4 sensillum housing the Ir84a ORNs (ac4A) was identified in distal region of the antenna based on their responsiveness to phenylacetaldehyde and the responsiveness of the neighboring neurons to phenylethylamine (Grosjean et al., 2011).

Odor stimuli—Phenylacetaldehyde was diluted in paraffin oil, applied as 100-μl aliquots on filter discs and delivered to the antenna via a 500-ms air pulse at 200 ml min^{-1} through the main airstream (2000 ml min^{-1}). Both *c*VA (10 μl per filer disc) and palmitoleic acid (4.5 μl per filer disc) were diluted in ethanol and delivered via a 500-ms air pulse at 250 ml min^{-1} directly to the antenna from a close range, as previously described (Ng et al., 2017). Ethanol was allowed to evaporate for 1 hour in a vacuum desiccator prior to experiments.

Immunohistochemistry—Two-day or seven-day old male files were anesthetized on ice, with their heads aligned in a collar, covered with Cryo-OCT (Tissue-Tek, Fisher Scientific), and frozen on dry ice as described (Saina and Benton, 2013). Cryosectioning was performed with CryoStar NX70 (Thermo Fisher Scientific) and 14-μm antennal sections were collected on Superfrost Plus microscope slides (Fisher Sceintific). Sections were fixed with 4% paraformaldehyde in phosphate-buffered saline (PBS) for 10 minutes, washed in PBST (PBS with 0.3% Triton X-100) for 3 minutes three times, and incubated for 30 minutes in the blocking solution (PBST with 5% normal goat serum). All steps were performed at room temperature unless otherwise noted. Myc-tag epitopes were labeled with rabbit anti-myc antibodies (1: 250 in the blocking solution, 71D10, Cell Signaling Technology) at 4°C overnight. After being washed three times in PBST, sections were incubated with the goat anti-rabbit Alexa 647 secondary antibody (1: 200 in the blocking solution, A21236, Life Technologies) for 2 hours at 4°C temperature, followed by 3×3 minutes washing in PBST. The sections were then mounted in DAPI Flouromount-G (Fisher Scientific). Confocal microscopy was performed with a Zeiss 880 Airyscan Microscope, and images were processed with ImageJ. As negative controls, parallel experiments were also conducted with 7-day old females, and the samples were imaged with identical acquisition parameters. Compared to male samples, only very faint myc staining signals were observed in females

and were therefore considered as background. For the analysis of male samples, the pixel value of myc staining within a neuron has to exceed the background level to be considered as positive signals.

Data analysis was performed in ImageJ. Briefly, ROIs were selected based on GFP labeling (as shown in Figure 3), and the fluorescence intensity of α-myc staining within individual ROIs was measured. Parallel experiments with identical image acquisition parameters were performed with 2-day and 7-day old males. This analysis aims to assay the relative up- or down-regulation of Fru^M isoforms in each age group, instead of the absolute levels of their expression.

Generation of *UAS-Fru^M* constructs—Three different *UAS-fru^M* constructs were made from *fru* male cDNA templates (Billeter et al., 2006b) by PCR amplification using the following primers (*fru* sequences shown in bold): shared forward primer FruMale_fwd (5′-TCT GAA TAG GGA ATT GGG AAT TC**A TGA TGG CGA CGT CAC AG**-3′) and isoform-specific reverse primers: FruA_rev (5′-GAT CCT CTA GAG GTA CCC TCG AG**T CAC ATA TGT ACA TAG TGG C**-3′); FruB_rev (5′-GAT CCT CTA GAG GTA CCC TCG AG**C TAC TCC TGC TGC CTT TTG**-3′); FruC_rev (5′- GAT CCT CTA GAG GTA CCC TCG AG**C TAC TAG TTT GGG TTA TGG TTA TTG**-3′). The resulting *fru^M* isoform DNA fragments were cloned into *EcoRI/XhoI* digested *pUASTattB* (Bischof et al., 2007) using Gibson Assembly® (NEB Cat. No. E2611S). Final constructs were confirmed by sequence analysis prior to insertion at the VK00033 docking site (Bloomington 9750; Venken et al., 2006).

Whole-mount brain imaging—Fly brains were dissected in ice cold PBS, fixed first in 4% (w/v) paraformaldehyde and then in 4% (w/v) paraformaldehyde containing 0.25% Triton X-100. Fixation was facilitated by microwaving the samples on ice for 1 min, repeated three times for each fixative. Samples were then placed in PBS and degassed in a vacuum chamber for 10 minutes. This step was repeated three times to remove air in the trachea. Samples were mounted in FocusClear™ (Cedarlane Labs, Canada) before native GFP was imaged for quantification. Samples were processed and imaged on the same day immediately after mounting. Images were acquired with a Zeiss LSM510 confocal microscope and a 40X/1.2 objective using the same laser power and detector gain for samples processed in parallel experiments.

Glomerular volumes were analyzed using ImageJ (NIH). Briefly, the stack range for the glomerulus of interest (i.e., 2–54 out of the 120 acquired images) was first identified. The contours of the VA1lm and DA1 glomeruli were manually traced in every five serial images until the entire glomerular volume was covered. The VL2a glomerulus, which is smaller than the other two glomeruli, was traced in every image instead. Glomerular sizes were then estimated by summing the area within each glomerular contour. To calculate the sex ratio, the glomerular volume of each male sample was divided by the average volume of the corresponding glomerulus in females.

Fru^M isoform binding motif alignment—The DNA sequences of the *ppk25* and *ppk23* genes, as well as the corresponding 5' region (2 kb), were obtained from FlyBase (https://

flybase.org/). Published Fru^M isoform binding motifs (Dalton et al., 2013; Neville et al., 2014) were used as queries to identify putative isoform-specific binding sites through sequence alignment using Serial Cloner 2.6 (http://serialbasics.free.fr/Serial_Cloner.html).

QUANTIFICATION AND STATISTICAL ANALYSIS

Statistics—Statistical results (p value and n) are indicated in figure legends corresponding to each experiment. In cases where a dosage curve for odor concentration was performed, two-tailed t tests comparing the experimental and control groups were performed for each concentration and the p- value is indicated on the figure by asterisks (*p < 0.05; **p < 0.01; ***p < 0.001). In cases where quantification of peak spike responses from each neuron was shown, two-way ANOVA followed by Tukey's post hoc test was performed in RStudio (https://www.rstudio.com), and p < 0.05 was considered statistically significant. To determine whether age influences the expression of Fru^M isoforms in target ORNs (Figures 3 and S2), two-sample t test was performed in RStudio to test whether the difference between two data populations (2-day and 7-day) is statistically different (p < 0.05). All graphs are plotted in Igor Pro 6.32A (https://www.wavemetrics.com/products/igorpro/igorpro). Dosage response curves were fitted with the Hill equation.

Supplementary Material

Refer to Web version on PubMed Central for supplementary material.

ACKOWLEDGMENTS

REFERENCES

Billeter JC, Rideout EJ, Dornan AJ, and Goodwin SF (2006a). Control of Male Sexual Behavior in Drosophila by the Sex Determination Pathway. Curr. Biol. 16, 766–776.

Billeter JC, Villella A, Allendorfer JB, Dornan AJ, Richardson M, Gailey DA, and Goodwin SF (2006b). Isoform-Specific Control of Male Neuronal Differentiation and Behavior in Drosophila by the fruitless Gene. Curr. Biol. 16, 1063–1076. [PubMed: 16753560]

Bischof J, Maeda RK, Hediger M, Karch F and Basler K (2007) An optimized transgenesis system for *Drosophila* using germ-line-specific phiC31 integrases. Proc. Natl. Acad. Sci. U.S.A. 104, 3312–3317. [PubMed: 17360644]

Chowdhury ZS, Sato K, and Yamamoto D (2017). The core-promoter factor TRF2 mediates a Fruitless action to masculinize neurobehavioral traits in Drosophila. Nat. Commun. 8, 1480. [PubMed: 29133872]

Dalton JE, Fear JM, Knott S, Baker BS, McIntyre LM, and Arbeitman MN (2013). Male-specific Fruitless isoforms have different regulatory roles conferred by distinct zinc finger DNA binding domains. BMC Genomics 14, 659. [PubMed: 24074028]

Demir E, and Dickson BJ (2005). fruitless splicing specifies male courtship behavior in Drosophila. Cell 121, 785–794. [PubMed: 15935764]

Dey S, Chamero P, Pru JK, Chien MS, Ibarra-Soria X, Spencer KR, Logan DW, Matsunami H, Peluso JJ, and Stowers L (2015). Cyclic regulation of sensory perception by a female hormone alters behavior. Cell 161, 1334–1344. [PubMed: 26046438]

Dickson BJ (2008). Wired for sex: the neurobiology of Drosophila mating decisions. Science. 322, 904–909. [PubMed: 18988843]

van der Goes van Naters W, and Carlson JR (2007). Receptors and Neurons for Fly Odors in Drosophila. Curr. Biol. 17, 606–612. [PubMed: 17363256]

Grosjean Y, Rytz R, Farine J-P, Abuin L, Cortot J, Jefferis GSXE, and Benton R (2011). An olfactory receptor for food-derived odours promotes male courtship in Drosophila. Nature 478, 236–240. [PubMed: 21964331]

Hanukoglu I, and Hanukoglu A (2016). Epithelial sodium channel (ENaC) family: Phylogeny, structure-function, tissue distribution, and associated inherited diseases. Gene 579, 95–132. [PubMed: 26772908]

Hueston CE, Olsen D, Li Q, Okuwa S, Peng B, Wu J, and Volkan PC (2016). Chromatin Modulatory Proteins and Olfactory Receptor Signaling in the Refinement and Maintenance of Fruitless Expression in Olfactory Receptor Neurons. PLOS Biol. 14, e1002443. [PubMed: 27093619]

Ito H, Sato K, Koganezawa M, Ote M, Matsumoto K, Hama C, and Yamamoto D (2012). Fruitless recruits two antagonistic chromatin factors to establish single-neuron sexual dimorphism. Cell 149, 1327–1338. [PubMed: 22682252]

Ito H, Sato K, Kondo S, Ueda R, and Yamamoto D (2016). Fruitless Represses robo1 Transcription to Shape Male-Speci fi c Neural Morphology and Behavior in Drosophila. Curr. Biol. 26, 1532–1542. [PubMed: 27265393]

Jindra M, Palli SR, and Riddiford LM (2013). The Juvenile Hormone Signaling Pathway in Insect Development. Annu. Rev. Entomol. 58, 181–204. [PubMed: 22994547]

Kaissling KE, Thorson J (1980). Insect olfactory sensilla: Structure, chemical and electrical aspect of the functional organization.

Kellenberger S, and Schild L (2002). Epithelial sodium channel/Degenerin family of ion channels: A variety of functions for a shared structure. Physiol. Rev. 82, 735–767. [PubMed: 12087134]

Knecht ZA, Silbering AF, Ni L, Klein M, Budelli G, Bell R, Abuin L, Ferrer AJ, Samuel ADT, Benton R, et al. (2016). Distinct combinations of variant ionotropic glutamate receptors mediate thermosensation and hygrosensation in Drosophila. Elife 5, e17879. [PubMed: 27656904]

Kurtovic A, Widmer A, and Dickson BJ (2007). A single class of olfactory neurons mediates behavioural responses to a Drosophila sex pheromone. Nature 446, 542–546. [PubMed: 17392786]

Lee G, and Hall JC (2001). Abnormalities of male-specific FRU protein and serotonin expression in the CNS of fruitless mutants in Drosophila. J. Neurosci. 21, 513–526. [PubMed: 11160431]

Lin H, Mann KJ, Starostina E, Kinser RD, and Pikielny CW (2005). A Drosophila DEG/ENaC channel subunit is required for male response to female pheromones. Proc. Natl. Acad. Sci. U. S. A. 102, 12831–12836. [PubMed: 16129837]

Lin H-H, Cao D-S, Sethi S, Zeng Z, Chin JSR, Chakraborty TS, Shepherd AK, Nguyen CA, Yew JY, Su C-Y, et al. (2016). Hormonal modulation of pheromone detection enhances male courtship success. Neuron 90, 1272–1285. [PubMed: 27263969]

Liu T, Wang Y, Tian Y, Zhang J, Zhao J, and Guo A (2018). The receptor channel formed by ppk25, ppk29 and ppk23 can sense the Drosophila female pheromone 7,11-heptacosadiene. Genes, Brain Behav. 1–10.

Meissner GW, Luo SD, Dias BG, Texada MJ, and Baker BS (2016). Sex-specific regulation of Lgr3 in Drosophila neurons. Proc. Natl. Acad. Sci. 113, E1256–E1265. [PubMed: 26884206]

Menuz K, Larter NK, Park J, and Carlson JR (2014). An RNA-Seq Screen of the Drosophila Antenna Identifies a Transporter Necessary for Ammonia Detection. PLoS Genet. 10, e1004810. [PubMed: 25412082]

Neville MC, Nojima T, Ashley E, Parker DJ, Walker J, Southall T, Van de Sande B, Marques AC, Fischer B, Brand AH, et al. (2014). Male-Specific Fruitless Isoforms Target Neurodevelopmental Genes to Specify a Sexually Dimorphic Nervous System. Curr. Biol. 24, 229–241. [PubMed: 24440396]

Ng R, Lin H-H, Wang JW, and Su C-Y (2017). Electrophysiological recording from Drosophila trichoid sensilla in response to odorants of low volatility. J. Vis. Exp. e56147.

Ng R, Salem SS, Wu S-T, Wu M, Lin H, Shepherd AK, Joiner WJ, Wang JW, and Su C (2019). Amplification of Drosophila Olfactory Responses by a DEG/ENaC Channel. Neuron 104, 947–959. [PubMed: 31629603]

Nojima T, Neville MC, and Goodwin SF (2014). Fruitless isoforms and target genes specify the sexually dimorphic nervous system underlying Drosophila reproductive behavior. Fly (Austin). 8, 95–100. [PubMed: 25483248]

Pavlou HJ, and Goodwin SF (2013). Courtship behavior in Drosophila melanogaster: Towards a "courtship connectome." Curr. Opin. Neurobiol. 23, 76–83. [PubMed: 23021897]

von Philipsborn AC, Jörchel S, Tirian L, Demir E, Morita T, Stern DL, and Dickson BJ (2014). Cellular and behavioral functions of fruitless isoforms in Drosophila courtship. Curr. Biol. 24, 242–251. [PubMed: 24440391]

Pikielny CW (2012). Sexy DEG/ENaC channels involved in gustatory detection of fruit fly pheromones. Sci. Signal. 5, p e48.

Ryner LC, Goodwin SF, Castrillon DH, Anand A, Villella A, Baker BS, Hall JC, Taylor BJ, and Wasserman SA (1996). Control of male sexual behavior and sexual orientation in Drosophila by the fruitless gene. Cell 87, 1079–1089. [PubMed: 8978612]

Saina M, and Benton R (2013). Visualizing olfactory receptor expression and localization in Drosophila. In Olfactory Receptors: Methods and Protocols, pp. 211–228.

Sato K, and Yamamoto D (2020). The mode of action of Fruitless: Is it an easy matter to switch the sex? Genes, Brain Behav. 19, e12606. [PubMed: 31420927]

Sato K, Ito H, Yokoyama A, Toba G, and Yamamoto D (2019). Partial proteasomal degradation of Lola triggers the male-to-female switch of a dimorphic courtship circuit. Nat. Commun. 10, 166. [PubMed: 30635583]

Sato K, Tanaka R, Ishikawa Y, and Yamamoto D (2020). Behavioral Evolution of Drosophila: Unraveling the Circuit Basis. Genes (Basel). 11, 157.

Sethi S, Lin H, Shepherd AK, Volkan PC, Su C, and Wang JW (2019). Social Context Enhances Hormonal Modulation of Pheromone Detection in Drosophila. Curr. Biol. 29, 3887–3898. [PubMed: 31679932]

Song HJ, Billeter JC, Reynaud E, Carlo T, Spana EP, Perrimon N, Goodwin SF, Baker BS, and Taylor BJ (2002). The fruitless gene is required for the proper formation of axonal tracts in the embryonic central nervous system of Drosophila. Genetics 162, 1703–1724. [PubMed: 12524343]

Starostina E, Liu T, Vijayan V, Zheng Z, Siwicki KK, and Pikielny CW (2012). A Drosophila DEG/ENaC subunit functions specifically in gustatory neurons required for male courtship behavior. J. Neurosci. 32, 4665–4674. [PubMed: 22457513]

Staruschenko A, Adams E, Booth RE, and Stockand JD (2005). Epithelial Na+ channel subunit stoichiometry. Biophys. J. 88, 3966–3975. [PubMed: 15821171]

Stockinger P, Kvitsiani D, Rotkopf S, Tirián L, and Dickson BJ (2005). Neural circuitry that governs Drosophila male courtship behavior. Cell 121, 795–807. [PubMed: 15935765]

Stogios PJ, Downs GS, Jauhal JJS, Nandra SK, and Privé GG (2005). Sequence and structural analysis of BTB domain proteins. Genome Biol. 6, 1–18.

Tal SH, and Smith DP (2006). A pheromone receptor mediates 11-cis-vaccenyl acetate-induced responses in Drosophila. J. Neurosci. 26, 8727–8733. [PubMed: 16928861]

Thistle R, Cameron P, Ghorayshi A, Dennison L, and Scott K (2012). Contact chemoreceptors mediate male-male repulsion and male-female attraction during Drosophila courtship. Cell 149, 1140–1151. [PubMed: 22632976]

Toda H, Zhao X, and Dickson BJ (2012). The Drosophila female aphrodisiac pheromone activates ppk23+ sensory neurons to elicit male courtship behavior. Cell Rep. 1, 599–607. [PubMed: 22813735]

Usui-Aoki K, Ito H, Ui-Tei K, Takahashi K, Lukacsovich T, Awano W, Nakata H, Piao ZF, Nilsson EE, Tomida J, et al. (2000). Formation of the male-specific muscle in female Drosophila by ectopic fruitless expression. Nat. Cell Biol. 2, 500–506. [PubMed: 10934470]

Vernes SC (2014). Genome wide identification of Fruitless targets suggests a role in upregulating genes important for neural circuit formation. Sci. Rep. 4, 1–11.

Venken KJ, He Y, Hoskins RA, and Bellen HJ (2006) P[acman]: a BAC transgenic platform for targeted insertion of large DNA fragments in *D. melanogaster*. Science 314,1747–1751. [PubMed: 17138868]

Vijayan V, Thistle R, Liu T, Starostina E, and Pikielny CW (2014). Drosophila pheromone-sensing neurons expressing the ppk25 ion channel subunit stimulate male courtship and female receptivity. PLoS Genet. 10, e1004238. [PubMed: 24675786]

Wang JW, Wong AM, Flores J, Vosshall LB, and Axel R (2003). Two-photon calcium imaging reveals an odor-evoked map of activity in the fly brain. Cell 112, 271–282. [PubMed: 12553914]

Wilson TG, and Fabian J (1986). A Drosophila melanogaster mutant resistant to a chemical analog of juvenile hormone. Dev. Biol. 118, 190–201. [PubMed: 3095161]

Wilson TG, DeMoor S, and Lei J (2003). Juvenile hormone involvement in Drosophila melanogaster male reproduction as suggested by the Methoprene-tolerant27 mutant phenotype. Insect Biochem. Mol. Biol. 33, 1167–1175. [PubMed: 14599489]

Wohl M, Ishii K, and Asahina K (2020). Layered roles of fruitless isoforms in specification and function of male aggression-promoting neurons in Drosophila. Elife 9, 1–31.

Yamamoto D, and Koganezawa M (2013). Genes and circuits of courtship behaviour in Drosophila males. Nat. Rev. Neurosci. 14, 681–692. [PubMed: 24052176]
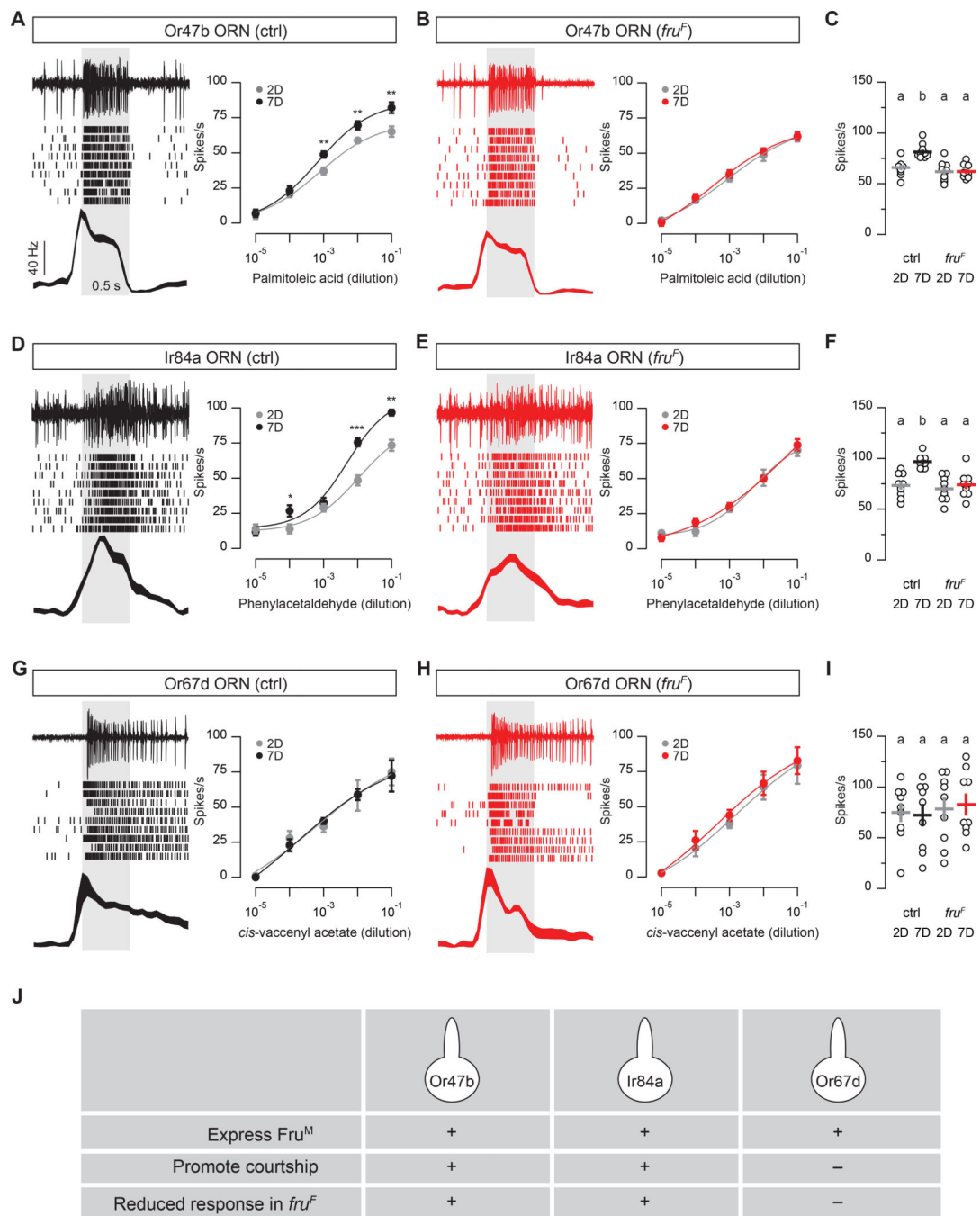
Figure 1. Fru^M is required for age-dependent olfactory sensitization

(A) Single-sensillum recording. Left panel: representative trace (top), rasters (middle), and peri-stimulus time histogram (PSTH; bottom) are shown for Or47b ORN responses in 7-day wildtype males (palmitoleic acid: 10^{-1}). Line width, SEM; gray bar, stimulus duration (0.5 s). Right panel: dosage curves of Or47b spike responses from 2-day and 7-day males. Adjusted peak responses (pre-stimulus baseline activity subtracted from peak response; see STAR Methods). Parallel experiments, mean ± SEM (n=9, from 4 flies). Significant

differences are denoted by *p < 0.05, **p < 0.01, ***p < 0.001 as determined by unpaired two-tailed t test.

(B) As in (A), but recordings instead performed in fru^F males.

(C) Quantification of Or47b ORN responses to palmitoleic acid (10^{-1}) in wildtype and fru^F males. Individual dots indicate responses from different neurons, from experiments shown in (A) and (B). Significant differences between any two groups (p < 0.05) are indicated by different letters; ANOVA followed by Tukey's test.

(D, E and F) As in (A), (B) and (C), but Ir84a ORN responses recorded instead from wildtype (D) or fru^F (E) males.

(G, H and I) As in (A), (B) and (C), but Or67d ORN responses recorded instead from wildtype (G) or fru^F (H) males.

(J) Fru^M is required for the age-dependent sensitization in the courtship-promoting ORNs.
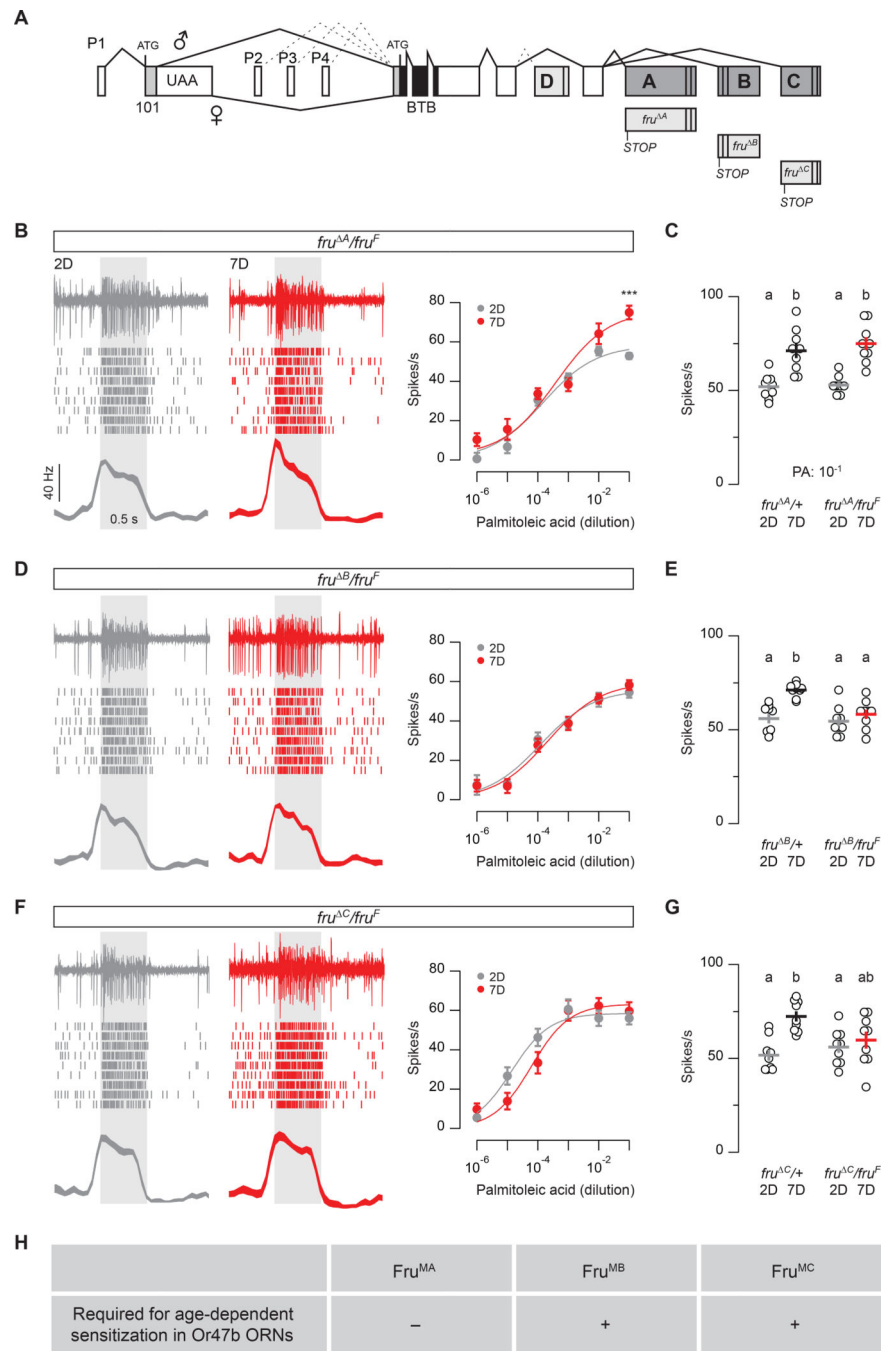
Figure 2. FruMB and FruMC are both required for the age-dependent sensitization of male Or47b neurons

(A) Schematics of the *fru* locus, adapted from Billeter et al., 2006b. P1–P4 indicate alternative promoters. The mRNA transcripts generated from the P1 promoter are spliced in a sexually-dimorphic manner, such that only males can produce functional Fru^M proteins. The BTB protein-protein interaction domain (black) and the A–C alternative exons encoding zinc-finger DNA binding domains (vertical black lines) are shown. Isoform-specific mutations are illustrated below.

(B) Single-sensillum recording from fru^{MA} mutant males (fru^{A}/fru^{F}). Sample traces, rasters, PSTHs (palmitoleic acid: 10^{-1}) and dosage curves are shown. Line width, SEM; gray bar, 0.5-s stimulus duration. Parallel experiments, mean $\pm$ SEM (n=9, from 4 flies). ***$p < 0.001$; t test.

(C) Quantification of Or47b ORN responses to palmitoleic acid (10^{-1}) from the indicated genotypes. Recordings were performed in parallel, mean $\pm$ SEM (n=9, from 4 flies). Significant differences between any two groups ($p < 0.05$) are indicated by different letters; ANOVA followed by Tukey's test.

(D–G) As in (B) and (C), recordings were instead performed in fru^{MB} mutants (D and E) or fru^{MC} mutants (F and G).

(H) Fru^{MB} and Fru^{MC} are both required for the age-dependent sensitization of Or47b ORNs.
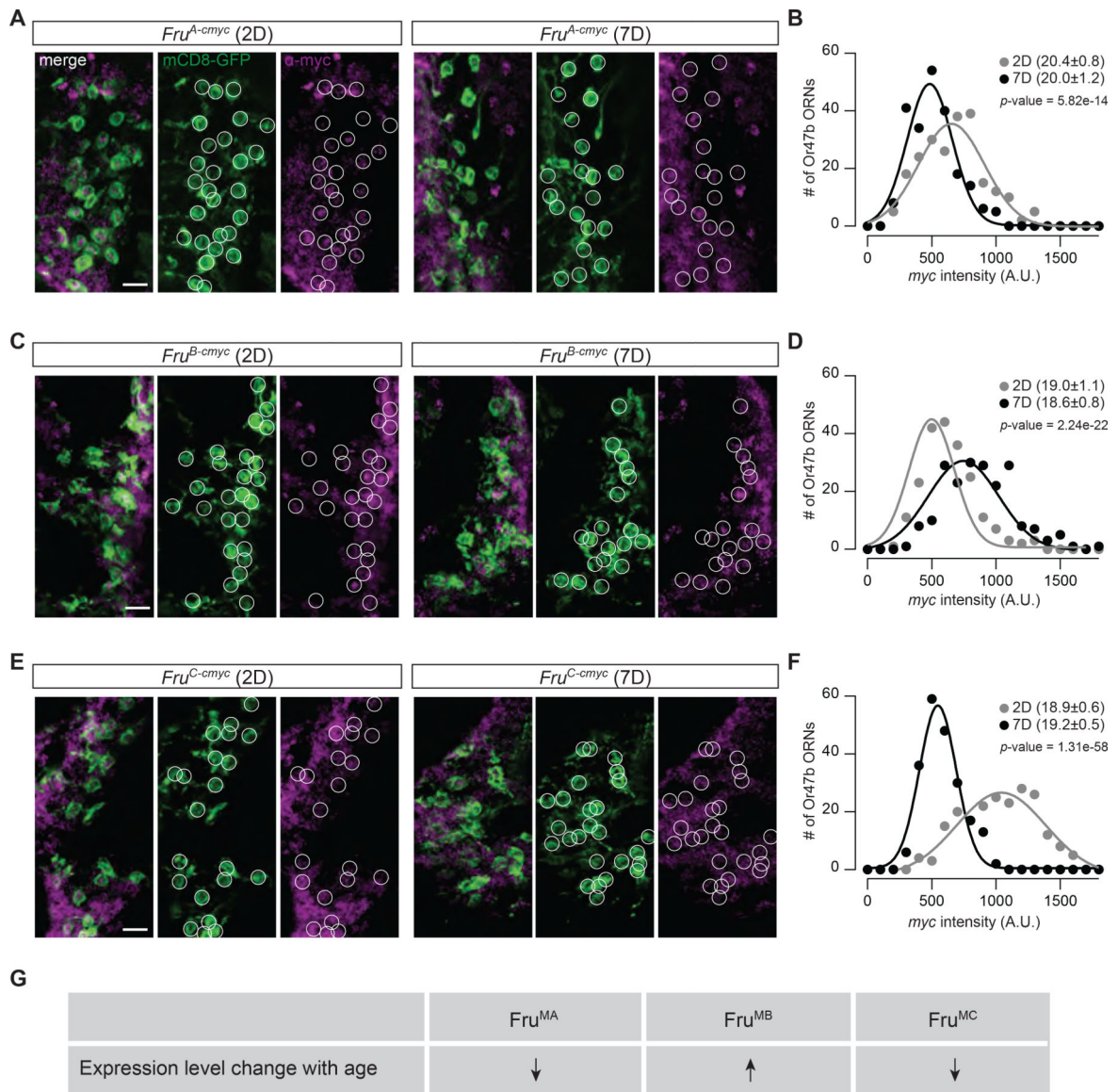
See also Figure S1.

Figure 3. Fru^M isoforms are differentially regulated by age in Or47b neurons

(A) Confocal images of antennal sections. GFP-labeled Or47b ORNs were outlined in circles (middle and right panels). Fru^{A-myc} was immunolabeled with anti-*myc* antibodies (α-myc, in magenta). Images were acquired with identical parameters in parallel experiments. Scale bar, 5 μm.

(B) Gaussian-fitted curves indicating the distribution of α-myc fluorescent levels in Or47b ORNs (data pooled from 11 antennal sections, one section per fly, data points binned at 100 A.U.). The average number of GFP-labeled Or47b neurons per antennal section is indicated in parentheses. Two-sample t test was applied to determine whether data distribution between age groups is significantly different.

(C–F) Similar to (A) and (B) except that Fru^{B-myc} (C and D) or Fru^{C-myc} (E and F) was immunolabeled and analyzed.

(G) In male Or47b ORNs, Fru^{MB} expression is upregulated with age, while Fru^{MA} and Fru^{MC} are downregulated.
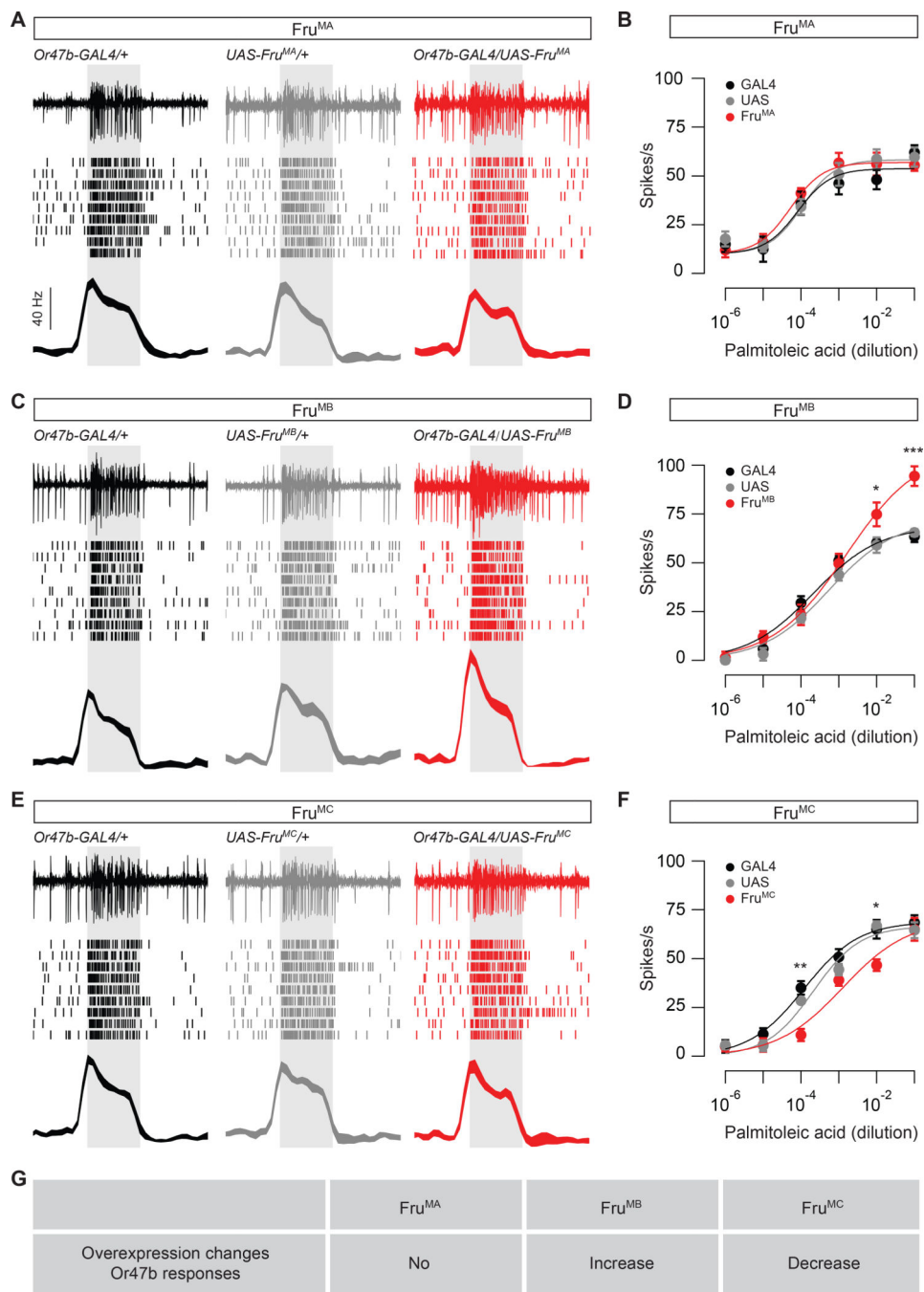
See also Figure S2.

Figure 4. Overexpression of Fru^MB elevates male Or47b ORN responses

(A) Single-sensillum recording. Representative traces (top), rasters (middle), and PSTHs (bottom) are shown for Or47b ORN responses in 2-day males (palmitoleic acid: 10^{-1}). Line width, SEM; gray bar, 0.5-s stimulus duration.

(B) Dosage curves of Or47b spike responses from controls and Fru^MA overexpression group (adjusted peak responses). Parallel experiments, mean $\pm$ SEM (n=9, from 4 flies for each genotype).

(C–F) Similar to (A) and (B) except that Fru^{MB} (C and D) or Fru^{MC} (E and F) was overexpressed. Significant differences are denoted by $*p < 0.05$, $**p < 0.01$, $***p < 0.001$ as determined by unpaired two-tailed t test.

(G) Upregulation of Fru^{MB}, but not Fru^{MA} or Fru^{MC}, increases Or47b olfactory responses in 2-day males.
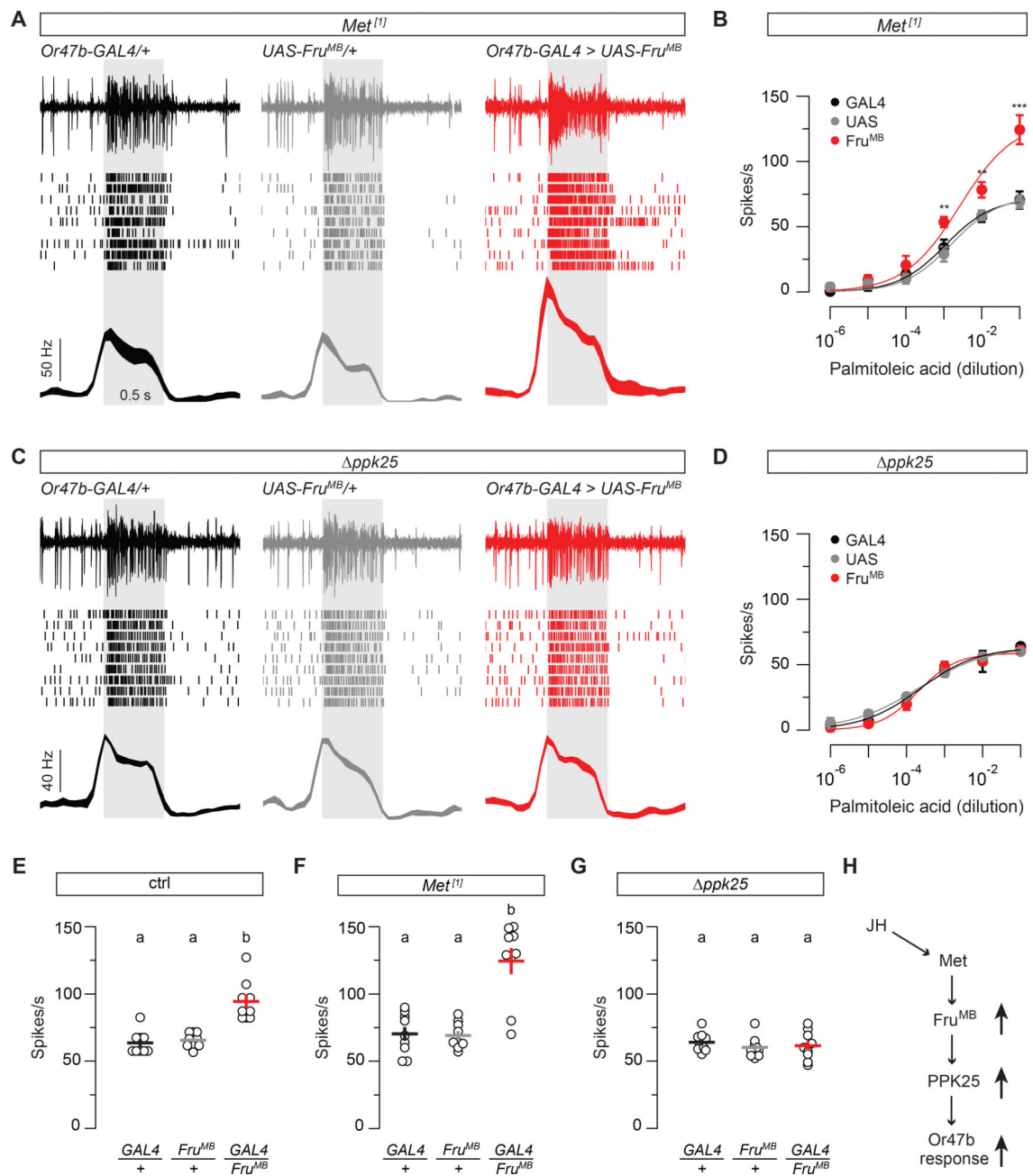
See also Figure S3.

Figure 5. Epitasis analysis of juvenile hormone signaling, Fru^MB and PPK25 in male Or47b ORNs

(A) Single-sensillum recording with 2-day old males in the *Met* mutant background (*Met[1]*). Representative traces (top), rasters (middle), and PSTHs (bottom) are shown for Or47b ORN responses from controls and Fru^MB overexpression males (palmitoleic acid: 10^{-1}). Line width, SEM; gray bar, 0.5-s stimulus duration.

(B) Dosage curves of Or47b ORN responses from controls and Fru^MB overexpression group (adjusted peak responses). Parallel experiments, mean ± SEM (n=9, from 4 flies for each genotype). Significant differences are denoted by **p < 0.01, ***p < 0.001 as determined by unpaired two-tailed t test.

(C and D) Similar to (A) and (B), recorded instead from 2-day old males in the *ppk25* mutant background (*ppk25*).

(E) Quantification of Or47b ORN responses to palmitoleic acid (10^{-1}) in 2-day old males. Same data points from Figure 4C. All flies were in wildtype background. Significant differences between any two groups ($p < 0.05$) are indicated by different letters; ANOVA followed by Tukey's test.

(F and G) Similar to (E), recorded instead from males in *ppk25* (F) or *Met* mutant background (G).

(H) Model based on epistasis analysis. In male Or47b neurons, juvenile hormone (JH) binds to its receptor, Methoprene-tolerant (Met), which increases Fru^{MB} expression in older males. Fru^{MB} in turn mediates PPK25 upregulation, thereby increasing Or47b neuronal response.
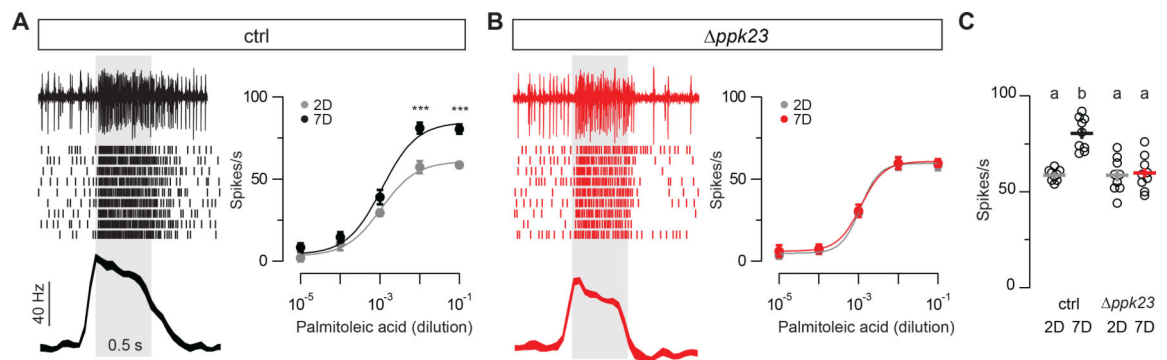
Figure 6. *ppk23* is required for Or47b neuronal sensitization

(A) Single-sensillum recording. Left panel: representative trace (top), raster plot (middle), and PSTH (bottom) are shown for Or47b ORN responses in 7-day wildtype males (palmitoleic acid: 10^{-1}). Line width, SEM; gray bar, 0.5-s stimulus duration. Right panel: dosage curves of Or47b spike responses from 2-day and 7-day males (adjusted peak responses). Parallel experiments, mean ± SEM (n=9, from 4 flies). ***$p < 0.001$; t test.

(B) As in (A), recordings instead performed from *ppk23* mutant males (Δ*ppk23*).

(C) Quantification of Or47b ORN responses to palmitoleic acid (10^{-1}) in wildtype or *ppk23* mutant males. Significant differences between any two groups ($p < 0.05$) are indicated by different letters; ANOVA followed by Tukey's test.
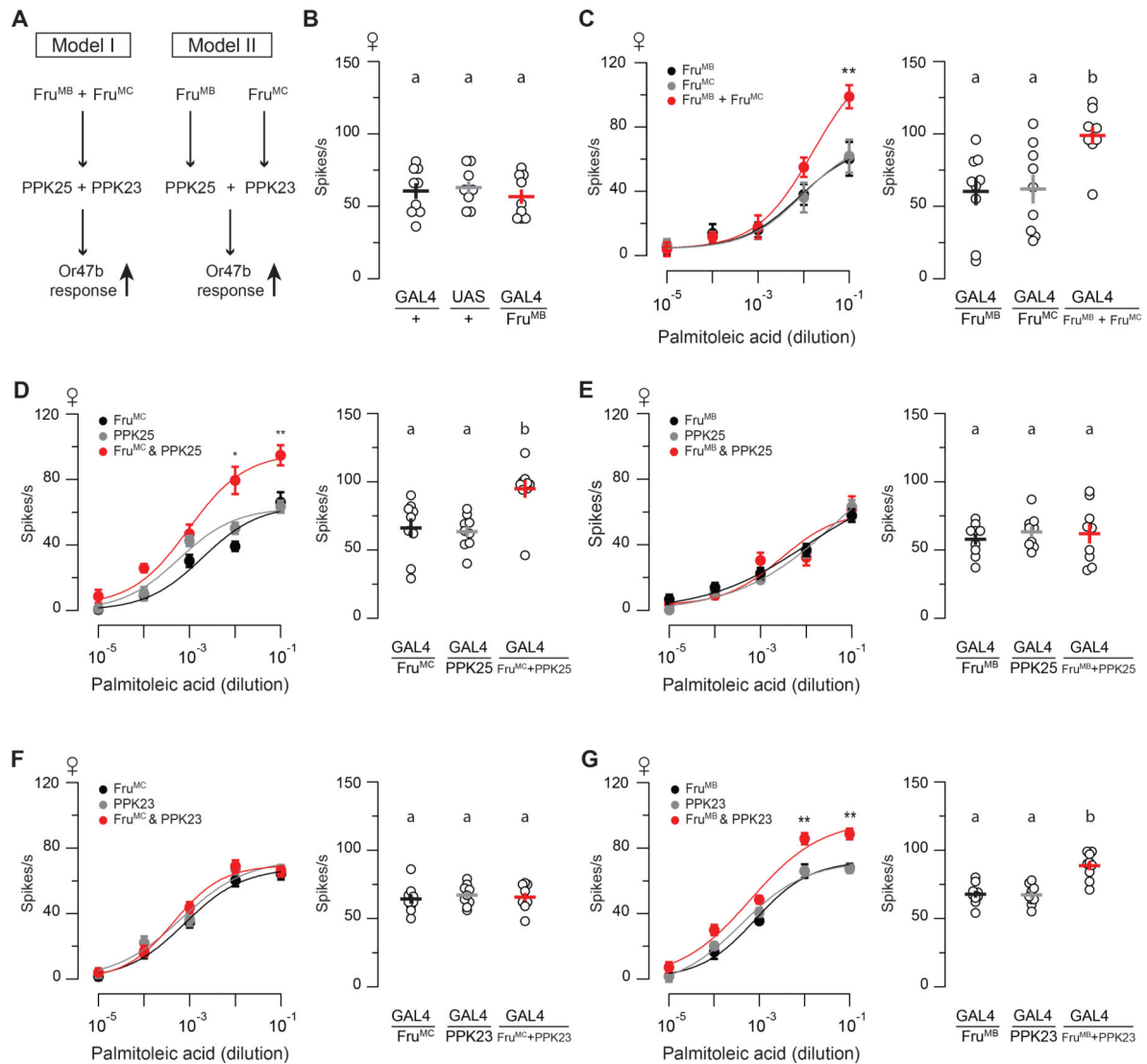
Figure 7. Fru^MB and Fru^MC cooperatively elevate Or47b ORN responses through distinct downstream effectors

(A) Working models. Model I: Fru^{MB} and Fru^{MC} require each other to mediate the expression of PPK25 and PPK23. Model II: Fru^{MB} and Fru^{MC} are upstream of distinct targets required for elevated Or47b ORN responses.

(B) Or47b ORN responses to palmitoleic acid (10^{-1}) from 2-day old virgin females of the indicated genotypes. Individual dots indicate data points from different neurons, lines represent mean ± SEM (n=9, from 4 flies, parallel experiments). ANOVA followed by Tukey's test.

(C) Or47b ORN responses from 2-day old virgin females expressing Fru^{MB}, Fru^{MC} or both isoforms. Dosage curves (left) and quantifications of the responses to palmitoleic acid (10^{-1}) (right) are shown. Parallel experiments, mean ± SEM (n=9, from 4 flies per genotype). Significant differences are indicated by asterisks (**p < 0.01; t test, left panel) or different letters (p < 0.05; ANOVA followed by Tukey's test; right panel).

(D) As in (C), recorded instead from female Or47b ORNs expressing PPK25, Fru^{MC} or both transgenes.

(E) As in (C), recorded instead from female Or47b ORNs expressing PPK25, Fru^{MB} or both transgenes.

(F) As in (C), recorded instead from female Or47b ORNs expressing PPK23, Fru^{MC} or both transgenes.

(G) As in (C), recorded instead from female Or47b ORNs expressing PPK23, Fru^{MB} or both transgenes.

See also Figures S4–S5.

KEY RESOURCES TABLE

REAGENT or RESOURCE	SOURCE	IDENTIFIER
Antibodies		
Myc-Tag (71D10) Rabbit mAB	Cell Signaling Technology	RRID:AB_10693332
Goat anti-Rabbit IgG (H+L) Cross-Adsorbed Secondary Antibody, Alexa Fluor 647	Invitrogen	RRID:AB_2535812
Chemicals (odorants)		
Phenylacetaldehyde	Sigma-Aldrich	122–78–1
trans-Palmitoleic Acid	Cayman Chemical	10030–73–6
11-*cis* Vaccenyl Acetate	Cayman Chemical	6186–98–7
Experimental Models: Organisms/Strains		
Drosophila: fru^F	Bloomington Stock Center	RRID:BDSC_66873
Drosophila: fru ^{A}	Neville et al., 2014	N/A
Drosophila: fru ^{B}	Neville et al., 2014	N/A
Drosophila: fru ^{C}	Billeter et al., 2006	N/A
Drosophila: Met$^{[1]}$	Wilson & Fabian, 1986	N/A
Drosophila: ppk25 $^{5–22}$	Lin et al., 2005	N/A
Drosophila: ppk23	Thistle et al., 2012, Cell	N/A
Drosophila: Fru^{A-myc}	von Philipsborn et al., 2014	N/A
Drosophila: Fru^{B-myc}	von Philipsborn et al., 2014	N/A
Drosophila: Fru^{C-myc}	von Philipsborn et al., 2014	N/A
Drosophila: Or47b-GAL4	Bloomington Stock Center	RRID:BDSC_9983
Drosophila: Or47b-GAL4	Bloomington Stock Center	RRID:BDSC_9984
Drosophila: Ir84a-GAL4	Bloomington Stock Center	RRID:BDSC_41734
Drosophila: Or67d-GAL4	Bloomington Stock Center	RRID:BDSC_9998
Drosophila: fru[GAL4.P1]	Bloomington Stock Center	RRID:BDSC_66696
Drosophila: UAS-PPK25	Vijayan et al., 2014	N/A
Drosophila: UAS-PPK23	Thistle et al., 2012	N/A
Drosophila: UAS-Fru^{MB}-shmiR	von Philipsborn Lab, Aarhus University	N/A
Drosophila: UAS-Fru^{MC}-shmiR	von Philipsborn et al., 2014	N/A
Drosophila: UAS-Fru^{MA}	Goodwin Lab, University of Oxford	N/A
Drosophila: UAS-Fru^{MB}	Goodwin Lab, University of Oxford	N/A
Drosophila: UAS-Fru^{MC}	Goodwin Lab, University of Oxford	N/A
Recombinant DNA		
Software and Algorithms		
ImageJ	NIH	https://imagej.nih.gov/ij/
Igor Pro 6.32A	WaveMetrics	https://www.wavemetrics.com/products/igorpro/igorpro
RStudio	Rstudio	https://www.rstudio.com

REAGENT or RESOURCE	SOURCE	IDENTIFIER
Clampfit 10.7	Molecular Devices	https://www.moleculardevices.com
Serial Cloner 2.6	Serial Basics	http://serialbasics.free.fr/Serial_Cloner.html
Other		
Aluminosilicate glass electrodes	Sutter Instrument Co., CA	AF100–64–10
Vacuum desiccator	Cole-Parmer, IL	VX-06514–30